Indian Journal of Pure & Applied Physics
Vol. 59, September 2021, pp. 619-628

Investigation to Enhance the DC and RF Performances of Nitride-Based Nanoelectronic HEMTs

Sanjib Kalita[a*], Avrajyoti Dutta[b] & Subhadeep Mukhopadhyay[b]

[a]Department of Electronics and Communication Engineering, Rajeev Gandhi Memorial College of Engineering and Technology, Nandyal, District–Kurnool, Andhra Pradesh — 518 501, India

[b]Department of Electronics and Communication Engineering, National Institute of Technology Arunachal Pradesh, Yupia, District-Papum Pare, Arunachal Pradesh — 791 112, India

Received 3 April 2021; accepted 30 July 2021

In this work, a structural optimisation is performed on the basis of DC and RF performances of high electron mobility transistors (HEMTs) in nano-scale regime by simulation results obtained from SILVACO-ATLAS physical simulator. The formation of quantum well is demonstrated at unbiased condition in each type of these HEMT structures. In DC analysis of each structure, the variations in drain current are studied with respect to drain voltage, gate voltage and doping concentration. Also, the variations in transconductance are studied with gate voltage and doping concentration corresponding to each structure. In RF analysis, the variations in current gain cut-off frequency and power gain cut-off frequency are studied with gate voltage and doping concentration corresponding to each structure. The DC and RF performances are observed to be the highest for modified HEMT structure with inserted InN atomic layer (0.36 nm thick) having AlGaN doping concentration of 4×10^{18} cm^{-3} among all designed structures in this work. To investigate the effect of doping concentration on DC and RF performances in nano-scale regime is one novelty in this work. Our work may be helpful in the applications related to biomedical sensors. Also, our work may be suitable for high frequency applications.

Keywords: Quantum well, Atomic layer, Doping concentration, Transconductance, Cut-off frequency

1 Introduction

From the last few years, the GaN-based HEMT has been thoroughly studied for its vast applications as high frequency and high power devices[1]. Apart from all GaN devices, for the presence of two-dimensional electron gas (2DEG), AlGaN/GaN HEMT attracts the attention of various research groups[2]. Recently, few authors have derived an analytical model on drain characteristics of GaN based single-heterojunction HEMTs[1]. According to that model, the drain current is higher at lower gate length in designed HEMT structures[1]. Chattopadhyay and Tokekar have developed another model on drain characteristics involving the effects of self-heating along with non-linear polarization in AlGaN/GaN HEMTs[2]. That analytical model shows good agreements with experimental results reported by other authors[2]. Also, Chattopadhyay and Tokekar have reported other analytical models on gate capacitance and transconductance related to GaN based single-heterojunction HEMTs[3, 4]. This model includes the effect of strain relaxation, donor neutralization and free carrier generation in the AlGaN layer.

Again, according to a charge-control model, GaN based single-heterojunction HEMTs may be used in microwave frequency applications[5]. In 2011, S Khandelwal *et al*. have presented a physics-based analytical model for 2-D electron gas density in AlGaN/GaN HEMTs[6]. Later on S Khandelwal *et al*. have reported many analytical models on GaN based single-heterojunction HEMTs related to intrinsic charge[7], surface potential[7], C-V characteristics[9], I-V characteristics[8], and gate current[8]. In 2013, Yigletu *et al*. have demonstrated a compact charge based model for current and capacitance of AlGaN/GaN HEMTs[10]. In the next year, Ghosh *et al*. have reported a gate current model of AlGaN/GaN HEMTs[11]. Also, they have reported the capacitance modelling of GaN based single-heterojunction HEMTs for proper switching behaviour[12]. Further, they have demonstrated one analytical model on GaN based HEMT for thermal noise[13]. Again, another model on 2DEG charge density has been derived related to GaAs HEMTs[14].

Corresponding author: (E-mail: sanjib.kalita25@gmail.com)

Recently, few authors have investigated the effects of mole fraction, doping concentration, gate length and nano-layer thickness on drain characteristics of single-heterojunction AlGaN/GaN HEMTs in Nanoelectronic regime[15, 16]. From these studies, higher drain currents have been observed in AlGaN/GaN HEMTs. Again, for higher current capability, nanoelectronic AlGaN/GaN HEMTs may be applicable to design and fabricate the biomedical sensors[17]. In 2018, Tai *et al*. developed a bio-sensor to screen for fibrinogen in clinical plasma samples using AlGaN/GaN HEMTs[18]. In the same year P Pal *et al*. have reported modelling and simulation of AlGaN/GaN HEMTs[19]. Recently, in 2020 Mishra *et al*. have designed a biomedical sensor using Normally-OFF AlGaN/GaN HEMTs[20].

Also, other simulation results are available to realise the electrical characteristics of HEMTs related to different semiconductor materials. In 2015, Miao *et al*. have introduced InN layer in the HMETs to increase the breakdown voltage[21]. Again, the effects of Al-mole fraction have been studied in AlGaN barried HEMT and GaN and InGaN channel HEMT with $In_{0.17}Al_{0.83}N$ barrier[22]. In 2019, Mohapatra *et al*. have studied high frequency performance of AlGaN/GaN HEMT with SiC substrate. From this, the author have obtain an extrinsic current gain cut-off frequency (F_T) of 78.9 GHz[32]. Therefore from all the above literatures, it has been observed that, it is very essential to study the effect of doping concentration on drain current, transconductance, current gain cut-off frequency and power gain cut-off frequency to get maximum device performance.

In this work, the drain characteristics of Nanoelectronic conventional single-heterojunction GaN based HEMTs along with modified Nanoelectronic GaN based HEMTs are studied with respect to drain voltage and gate voltage according to the DC analysis. Also, by the DC analysis, the variations in transconductance with gate voltage are studied in the designed HEMT structures. Variations in current gain cut-off frequency and power gain cut-off frequency with gate voltage are studied in the designed HEMT structures by the RF analysis. The effects of inserted aluminium nitride (AlN) atomic layer and inserted indium nitride (InN) atomic layer on DC and RF performances are investigated. According to the above mentioned systematically performed investigations, this study may be suitable for the research area related to biomedical sensors and high frequency applications.

2 Designs of Simulated Structures

2.1. Designs of conventional HEMTs

Figure 1 shows a representative designed-structure of conventional HEMTs. The ohmic positions of source, gate and drain are clearly shown in the schematic diagram. The widths of source, gate and drain are 150, 300 and 150 nm respectively. The distance between source and gate is 200 nm. The distance between gate and drain is 600 nm. For improving the breakdown voltage, the gate to drain distance is increased as compared to the gate to source distance. It has been reported that the breakdown voltage of HEMT depends on the gate to drain distance. As the gate to drain distance increases, the critical field for breakdown is obtained at higher drain voltage[23]. Again, by reducing the gate to source length, the electric field component along the channel enhanced providing an increase in carrier density under the gate[24]. A GaN cap layer having 1 nm of thickness is designed below the gate. An $Al_{0.3}Ga_{0.7}N$ nano-layer having 10 nm of thickness is designed below the cap layer. A GaN layer having 21 nm of thickness is designed below the $Al_{0.3}Ga_{0.7}N$ nano-layer. Another GaN layer having 48 nm of thickness is designed just above the sapphire substrate. Ga-faced GaN is used. Ga-faced GaN is more chemically inert than chemically active =N-faced GaN.

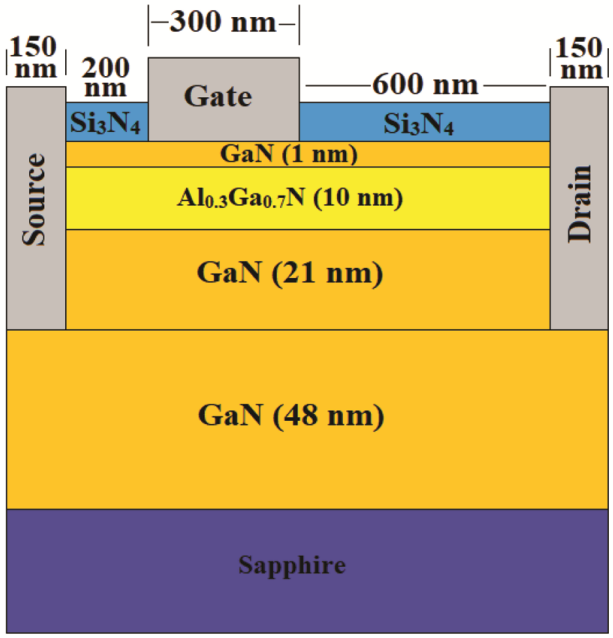

Fig. 1 — A representative schematic diagram of the Nanoelectronic GaN/AlGaN/GaN HEMTs is shown (cross-sectional view).

Now, Ga-faced GaN has a growth direction of [0001] according to the already published literature[25]. Total 4 individual conventional HEMTs are designed having distinction among each other due to different $Al_{0.3}Ga_{0.7}N$ doping concentrations. The doping concentrations of $Al_{0.3}Ga_{0.7}N$ layer in these designed-structures are 1×10^{18} cm^{-3}, 2×10^{18} cm^{-3}, 3×10^{18} cm^{-3}, and 4×10^{18} cm^{-3}.

2.2. Designs of HEMTs with inserted atomic layers

In Fig. 2, the conventional HEMT is modified only by inserting one aluminium nitride (AlN) atomic layer having 0.36 nm of thickness with the expectation of better DC and RF performances with respect to the conventional HEMT. Similarly, in Fig. 3, the conventional HEMT is separately modified only by inserting one indium nitride (InN) atomic layer having 0.36 nm of thickness with the expectation of better DC and RF performances than conventional HEMT. Due to the insertion of InN layer between the AlGaN and GaN layers, the mobility is increased and the high-frequency performance is improved[26]. It has been reported that the atomic layer of InN above the GaN layer produces high quality HEMT device as it reduces the defects due to the lattice mismatch between the layers[27]. Already many researchers have deposited atomic layers of different thickness using the plasma enhanced atomic layer deposition (PE-ALD) technique. The growth per cycle (GPC) for AlN is 0.6 Å/cycle and that for InN is 0.36 Å/cycle[28-30].

In this present simulation, 3.6 Å *i.e.* 0.36 nm is considered for AlN layer and for InN layer which can be grown above the GaN layer by depositing 6 cycles and 10 cycles for AlN and InN respectively using PE-ALD technique. Also, a comparison for better DC and RF performances can be made between the modified structures of Fig. 2 and Fig. 3.

In the category of modified HEMTs shown by Fig. 2, total 4 individual modified HEMTs are designed having distinction among each other due to different $Al_{0.3}Ga_{0.7}N$ doping concentrations. The doping concentrations of $Al_{0.3}Ga_{0.7}N$ nano-layer in these designed-structures of Fig. 2 are 1×10^{18} cm^{-3}, 2×10^{18} cm^{-3}, 3×10^{18} cm^{-3}, and 4×10^{18} cm^{-3}. In the category of modified HEMTs shown by Fig. 3, again, total 4 individual modified HEMTs are designed having distinction among each other due to different $Al_{0.3}Ga_{0.7}N$ doping concentrations. The doping concentrations of $Al_{0.3}Ga_{0.7}N$ nano-layer in these designed-structures of Fig. 3 are 1×10^{18} cm^{-3}, 2×10^{18} cm^{-3}, 3×10^{18} cm^{-3}, and 4×10^{18} cm^{-3}.

3 Models Used in Simulation

In this research paper, all the simulation results are obtained by the SILVACO-ATLAS physical simulator using the following models: Shockley Read Hall (SRH), Polarization model, field dependent mobility (FLDMOB), concentration dependent mobility (CONMOB), and Fermi Dirac statistics.

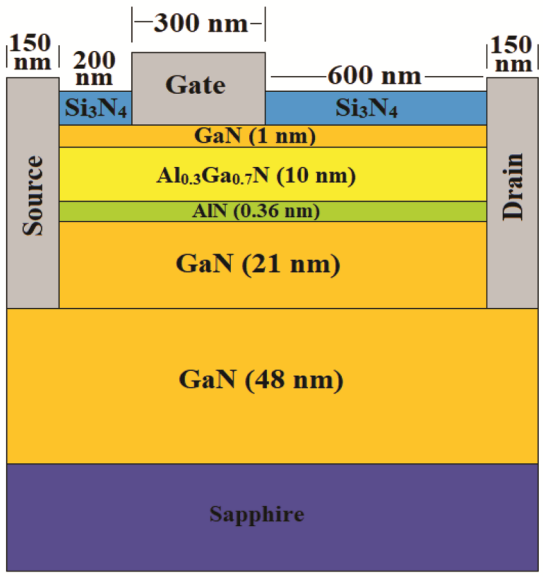

Fig. 2 — A representative schematic diagram of the Nanoelectronic GaN/AlGaN/AlN/GaN HEMTs is shown (cross-sectional view).

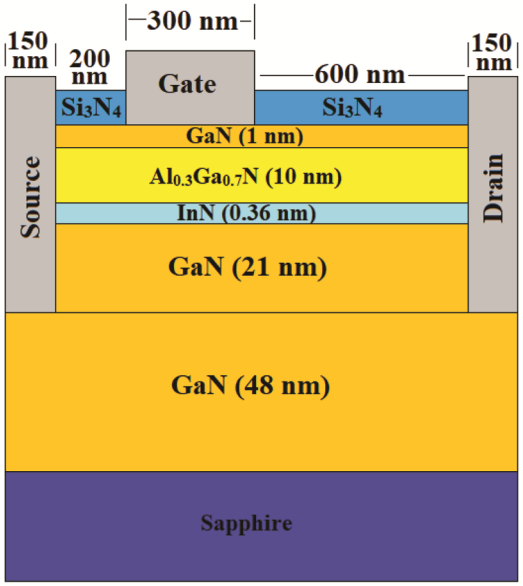

Fig. 3 — A representative schematic diagram of the Nanoelectronic GaN/AlGaN/InN/GaN HEMTs is shown (cross-sectional view).

Phonon transition occurs due to the defects in semiconductor. SRH model is used to account this phonon transition. Also, SRH model is used to represent the carrier generation-recombination process along with fixing the minority carrier lifetime. The calculation of field dependent mobility is used by specifying the FLDMOB in MODEL statement.

A polarisation model is used in SILVACO-ATLAS simulation. CALC.STRAIN syntax is used inside this polarisation model to calculate the following: (a) strain from the lattice mismatch, and (b) piezoelectric polarization. Again, POLAR.SCALE is used which specifies a constant scale factor multiplied by the calculated spontaneous polarisation and piezoelectric polarisation. The value of POLAR.SCALE is used as 0.8.

Again, FLDMOB model is used for high electric field velocity saturation in HEMT. The mobility due to doping concentration is calculated by specifying CONMOB in MODEL statement of SILVACO-ATLAS program. Again, lateral field mobility and standard concentration dependent mobility are specified by using Fermi-Dirac statistical model in simulation. It is a statistical approach to reduce the carrier concentration at heavily doped regions. POLARIZATION model is used to calculate the polarization charge density due to the presence of spontaneous polarization and piezoelectric polarization at AlGaN/GaN HEMT. The Newton-trap numerical solver is used in device simulation of this research paper.

4 Results and Discussion

4.1. DC and RF performances of conventional HEMTs at any particular AlGaN doping concentration

Figures 4 to 7 show the DC performance of conventional HEMTs having different AlGaN doping concentrations. Figure 4 shows the conduction band engineering of conventional GaN/AlGaN/GaN HEMT at AlGaN doping concentration of 2×10^{18} cm^{-3} to form the quantum well at heterojunction for electron confinement generating a two dimensional electron gas (2DEG). As, GaN is a narrow bang gap material compared to the AlGaN. Hence, at the hetero-interface between AlGaN and GaN, the conduction band bending is observed forming the quantum well. Figure 5 shows the variations of drain current with drain voltage at different fixed gate voltages, corresponding to the conventional HEMTs at different AlGaN doping concentrations[1,31]. According to Fig. 5,

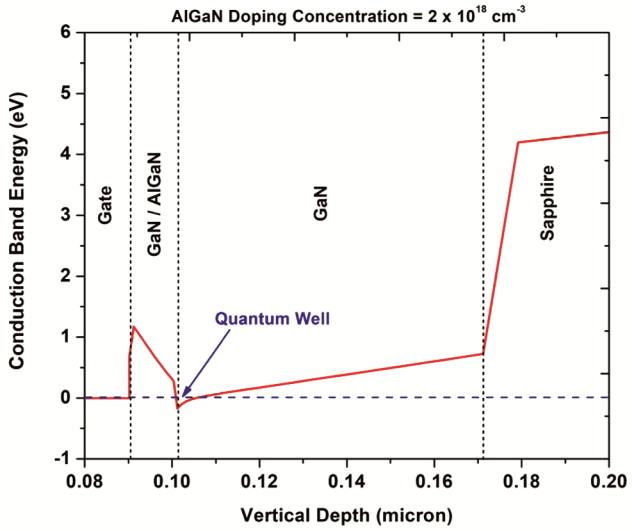

Fig. 4 — The formation of quantum well is directly demonstrated from SILVACO-ATLAS physical simulator for Nanoelectronic GaN/AlGaN/GaN HEMT at the AlGaN doping concentration of 2×10^{18} cm^{-3}. This quantum well is obtained at the unbiased condition.

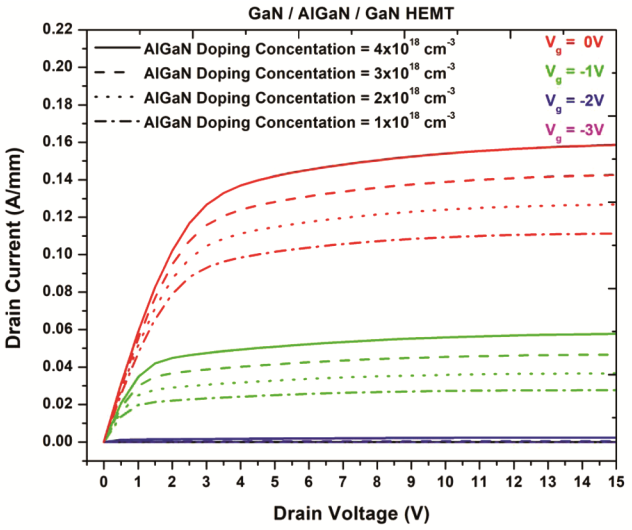

Fig. 5 — The variations in drain current with drain voltage are shown at different gate voltages for different AlGaN doping concentrations corresponding to GaN/AlGaN/GaN HEMTs.

the drain current increases with drain voltage at any particular fixed gate voltage (V_g) and at any particular AlGaN doping concentration[1, 31]. Also, the drain current is larger at higher gate voltage (V_g) at any particular AlGaN doping concentration[15,16]. As GaN/AlGaN/GaN HEMT is normally-ON device, the maximum drain current has been observed at a gate voltage of zero volt.

According to Fig. 6, the drain current is larger at higher gate voltage for fixed drain voltage (V_d) of 5

volt at any particular AlGaN doping concentration[15,16]. From this, a cutoff voltage of -2 volt has been observed. As mentioned earlier, this device is Normally-ON type, so, it will turn off only after giving negative voltage at gate terminal. Also, according to Fig. 7, the transconductance gets a peak around the gate voltage of 1 volt at any particular AlGaN doping concentration[22, 31]. Fig. 8 shows the RF performance of conventional HEMTs at fixed drain voltage (V_d) of 5 volt at any particular AlGaN doping concentration. According to Fig. 8, the current gain cut-off frequency (F_T) gets a peak around the gate voltages of 0 volt to 0.5 volt at any particular AlGaN doping concentration[31]. It has been observed that at a doping concentration of 4×10^{18} cm^{-3}, a current gain cut-off frequency of 90 GHz has been obtained. Also, according to Fig. 9, the power gain cut-off frequency (F_{max}) gets a peak around the gate voltages of 0 volt to 0.5 volt at any particular AlGaN doping concentration[31]. Here, a power gain cut-off frequency of 160 GHz has been observed at a doping concentration of 4×10^{18} cm^{-3}.

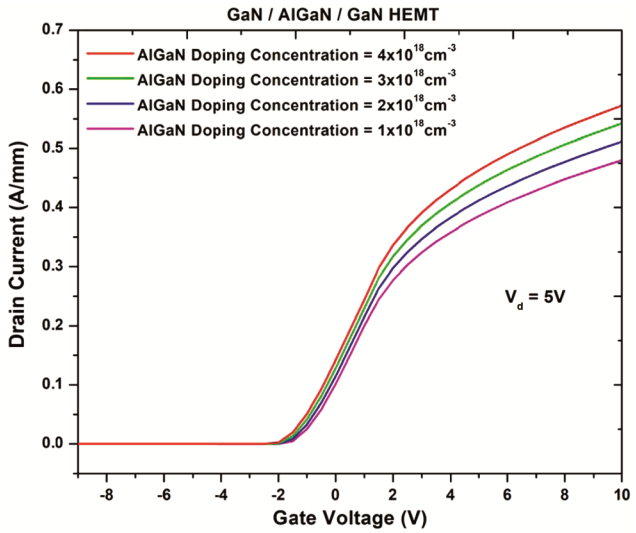

Fig. 6 — The variations in drain current with gate voltage are shown at the fixed drain voltage (V_d) of 5 volt for different AlGaN doping concentrations corresponding to GaN/AlGaN/GaN HEMTs.

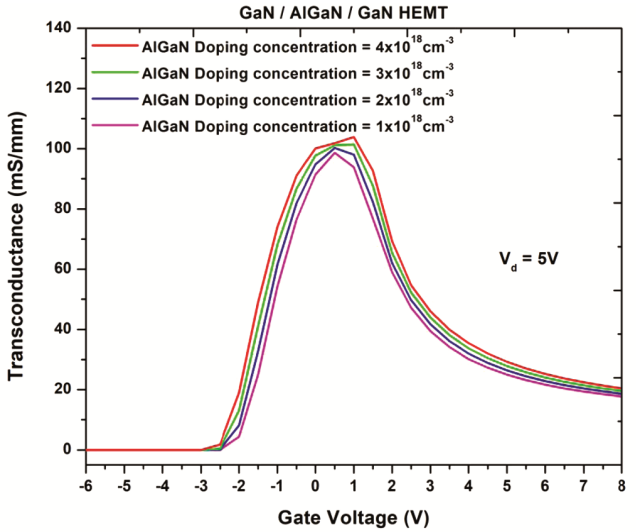

Fig. 7 — The variations in transconductance with gate voltage are shown at the fixed drain voltage (V_d) of 5 volt for different AlGaN doping concentrations corresponding to GaN/AlGaN/GaN HEMTs.

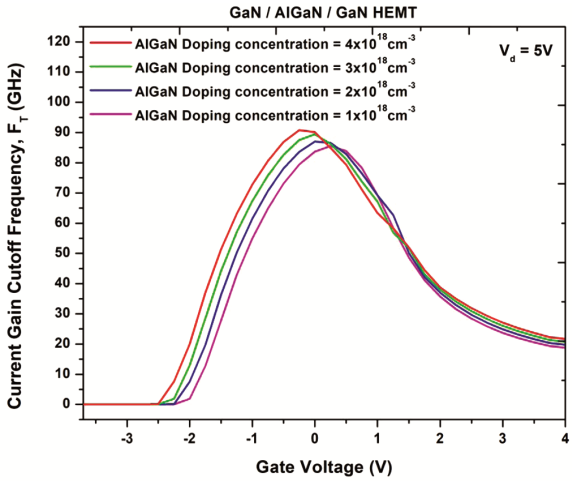

Fig. 8 — The variations in current gain cut-off frequency with gate voltage are shown at the fixed drain voltage (V_d) of 5 volt for different AlGaN doping concentrations corresponding to GaN/AlGaN/GaN HEMTs.

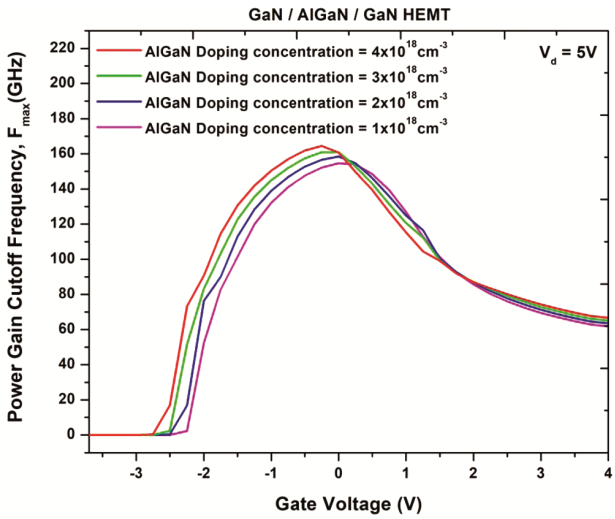

Fig. 9 — The variations in power gain cut-off frequency with gate voltage are shown at the fixed drain voltage (V_d) of 5 volt for different AlGaN doping concentrations corresponding to GaN/AlGaN/GaN HEMTs.

4.2. Effect of AlGaN doping concentration on DC and RF performances of conventional HEMTs

According to Fig. 5 and Fig. 6, the drain current is higher for higher AlGaN doping concentration of GaN/AlGaN/GaN HEMT at any particular combination of drain voltage and gate voltage[15, 16]. According to Fig. 7, the transconductance is higher for larger AlGaN doping concentration of GaN/AlGaN/GaN HEMT at any particular gate voltage corresponding to the fixed drain voltage (V_d) of 5 volt. According to Fig. 8, the current gain cut-off frequency (F_T) is higher for larger AlGaN doping concentration of GaN/AlGaN/GaN HEMTs at any particular gate voltage corresponding to the fixed drain voltage (V_d) of 5 volt. According to Fig. 9, the power gain cut-off frequency (F_{max}) is higher for larger AlGaN doping concentration of GaN/AlGaN/GaN HEMTs at any particular gate voltage corresponding to the fixed drain voltage (V_d) of 5 volt.

4.3. DC and RF performances of HEMTs with inserted atomic layers

Figure 10 shows the formation of quantum well in modified HEMT structure with inserted AlN atomic layer, to generate the 2DEG. Due to the large band gap of AlN layer, increased conduction band discontinuity has been observed at the junction of AlN and GaN layer. Hence, the depth of the quantum well is slightly increased resulting into the increase in 2DEG density. Fig. 11 to Fig. 15 show the DC and RF performances of GaN/AlGaN/AlN/GaN HEMTs. Fig. 11 and Fig. 12 show the increasing drain current with drain voltage for any particular gate voltage at any particular AlGaN doping concentration corresponding to the structure with inserted AlN atomic layer[22]. For higher 2DEG density slight increase drain currents have been observed in this device than conventional HEMTs. Fig. 13 shows the variations in transconductance with gate voltage for the fixed drain voltage (V_d) of 5 volt at different AlGaN doping concentrations corresponding to GaN/AlGaN/AlN/GaN HEMTs. The transconductance gets a peak at the gate voltage of 0.5 volt for any particular AlGaN doping concentration corresponding to the GaN/AlGaN/AlN/GaN HEMTs.

Figure 14 shows the variations in current gain cut-off frequency with gate voltage at the fixed drain voltage (V_d) of 5 volt for different AlGaN doping concentrations corresponding to GaN/AlGaN/AlN/GaN HEMTs. The current gain cut-off frequency gets a peak at the gate voltages from 0.1 volt to 0.6 volt corresponding to different AlGaN doping concentrations. Figure 15 shows the variations in power gain cut-off frequency with gate voltage at the fixed drain voltage (V_d) of 5 volt for different AlGaN doping concentrations corresponding to GaN/AlGaN/AlN/GaN HEMTs. The power gain cut-off frequency gets a peak at the gate voltages from 0 volt to 0.5 volt corresponding to different AlGaN doping concentrations. From Fig. 14 and Fig.15, it have been observed that the current gain cut-off frequency and power gain cut-off frequency

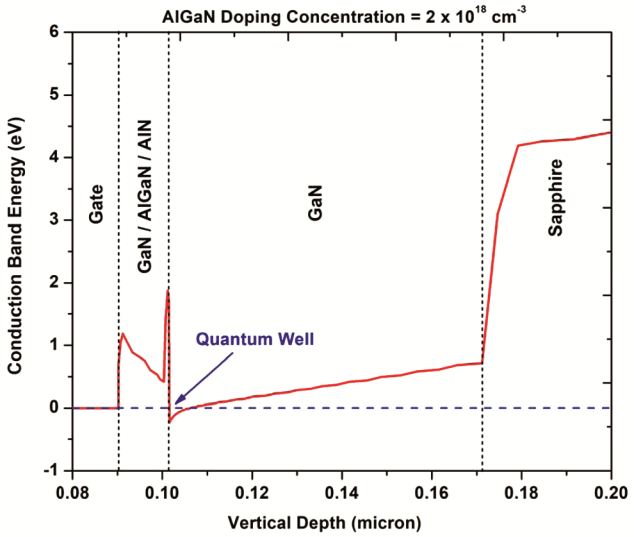

Fig. 10 — The formation of quantum well is directly demonstrated from SILVACO-ATLAS physical simulator for Nanoelectronic GaN/AlGaN/AlN/GaN HEMT at the AlGaN doping concentration of 2×10^{18} cm^{-3}. This quantum well is obtained at the unbiased condition.

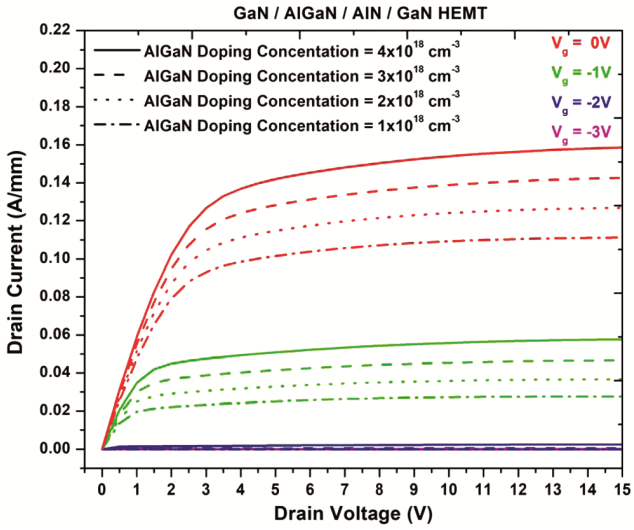

Fig. 11 — The variations in drain current with drain voltage are shown at different gate voltages for different AlGaN doping concentrations corresponding to GaN/AlGaN/AlN/GaN HEMTs.

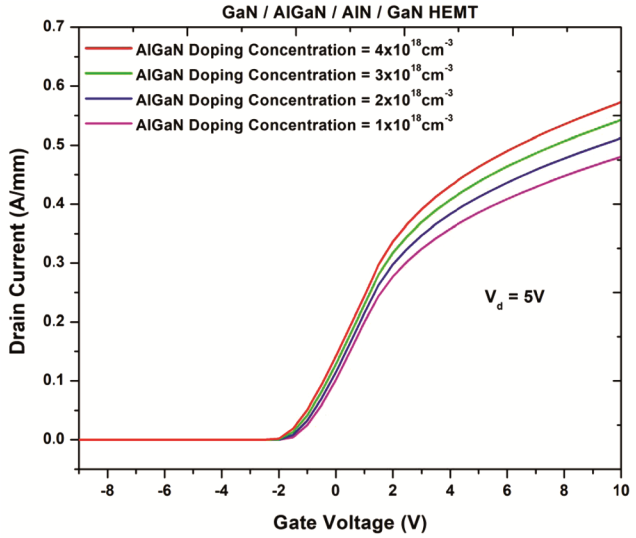

Fig. 12 — The variations in drain current with gate voltage are shown at the fixed drain voltage (V_d) of 5 volt for different AlGaN doping concentrations corresponding to GaN/AlGaN/AlN/GaN HEMTs.

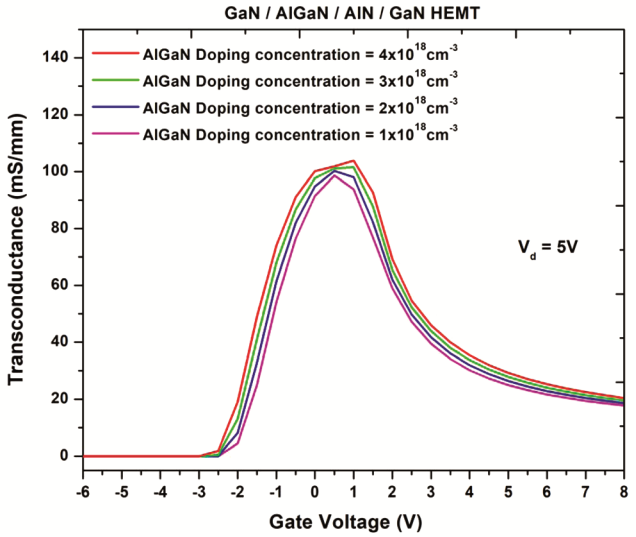

Fig. 13 — The variations in transconductance with gate voltage are shown at the fixed drain voltage (V_d) of 5 volt for different AlGaN doping concentrations corresponding to GaN/AlGaN/AlN/GaN HEMTs.

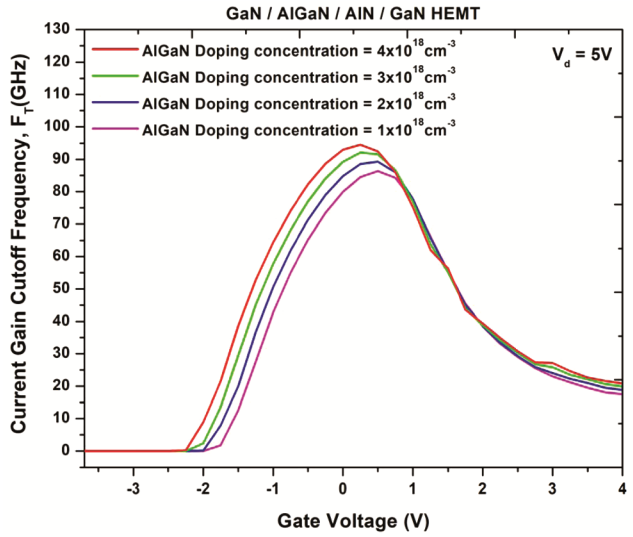

Fig. 14 — The variations in current gain cut-off frequency with gate voltage are shown at the fixed drain voltage (V_d) of 5 volt for different AlGaN doping concentrations corresponding to GaN/AlGaN/AlN/GaN HEMTs.

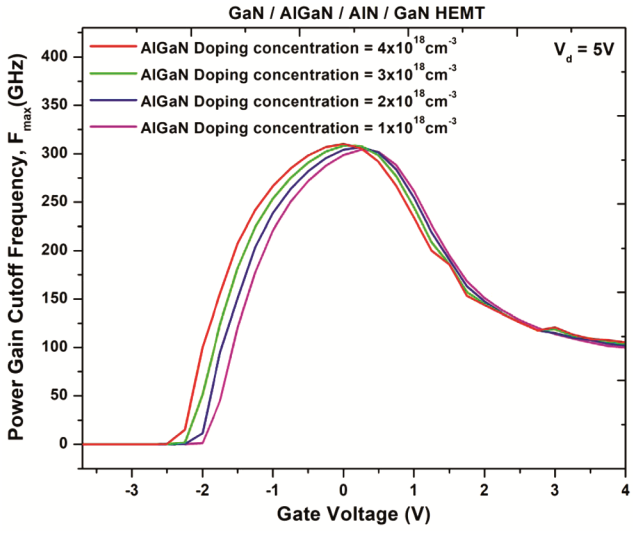

Fig. 15 — The variations in power gain cut-off frequency with gate voltage are shown at the fixed drain voltage (V_d) of 5 volt for different AlGaN doping concentrations corresponding to GaN/AlGaN/AlN/GaN HEMTs.

significantly increased due to the insertion of AlN atomic layer, which can be useful for high frequency applications.

Figure 16 shows the formation of quantum well in modified HEMT structure with inserted InN atomic layer, to generate the 2DEG. Here, deep and thin quantum well can be observed in the InN atomic layer, as the band gap of InN layer is very small. Again, Fig. 17 to Fig. 19 show the DC performance of GaN/AlGaN/InN/GaN HEMTs. Fig. 17 and Fig. 18 show the increasing drain current with drain voltage for any particular gate voltage at any particular AlGaN doping concentration corresponding to the structure with inserted InN atomic layer[22]. As per Fig. 16, the 2DEG density is increased due to the higher quantum well depth resulting higher drain current. For this reason, this type devices can be useful for biomedical sensor applications which will give the higher sensitivity[17]. Fig. 19 shows the variations in transconductance with gate voltage for the fixed drain

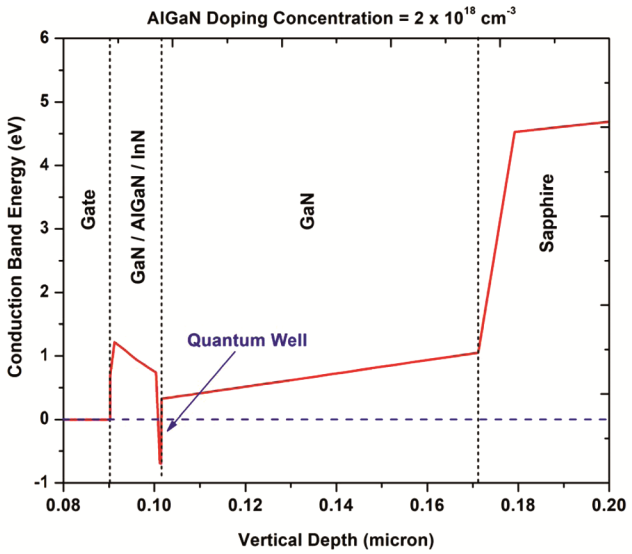

Fig. 16 — The formation of quantum well is directly demonstrated from SILVACO-ATLAS physical simulator for Nanoelectronic GaN/AlGaN/InN/GaN HEMT at the AlGaN doping concentration of 2×10^{18} cm^{-3}. This quantum well is obtained at the unbiased condition.

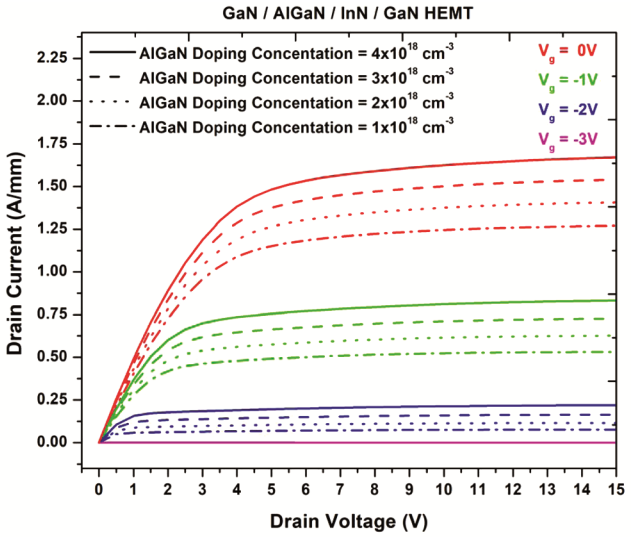

Fig. 17 — The variations in drain current with drain voltage are shown at different gate voltages for different AlGaN doping concentrations corresponding to GaN/AlGaN/InN/GaN HEMTs.

voltage (V_d) of 5 volt at different AlGaN doping concentrations corresponding to GaN/AlGaN/InN/GaN HEMTs. The transconductance gets a peak at the gate voltages from -0.8 volt to 0.4 volt at the fixed drain voltage (V_d) of 0.5 volt for any particular AlGaN doping concentration corresponding to the GaN/AlGaN/InN/GaN HEMTs.

Figure 20 shows the variations in current gain cut-off frequency with gate voltage at the fixed drain

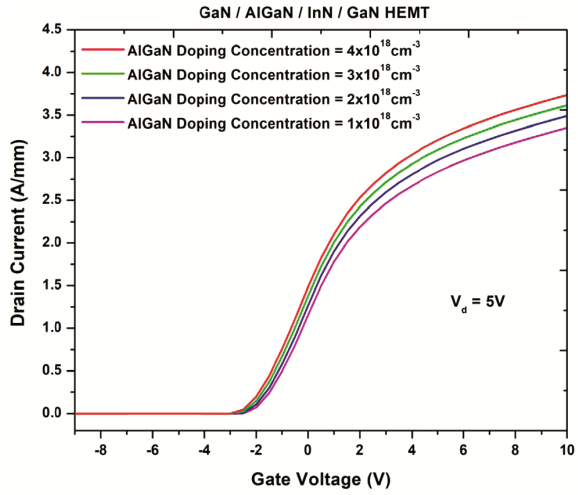

Fig. 18 — The variations in drain current with gate voltage are shown at the fixed drain voltage (V_d) of 5 volt for different AlGaN doping concentrations corresponding to GaN/AlGaN/InN/GaN HEMTs.

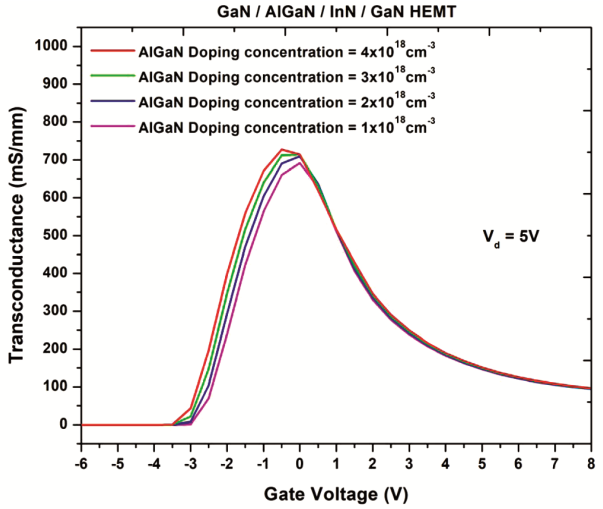

Fig. 19 — The variations in transconductance with gate voltage are shown at the fixed drain voltage (V_d) of 5 volt for different AlGaN doping concentrations corresponding to GaN/AlGaN/InN/GaN HEMTs.

voltage (V_d) of 5 volt for different AlGaN doping concentrations corresponding to GaN/AlGaN/InN/GaN HEMTs. The current gain cut-off frequency gets a peak at the gate voltages from -0.8 volt to - 0.2 volt corresponding to different AlGaN doping concentrations of GaN/AlGaN/InN/GaN HEMTs. Fig. 21 shows the variations in power gain cut-off frequency with gate voltage at the fixed drain voltage (V_d) of 5 volt for different AlGaN doping concentrations corresponding to GaN/AlGaN/InN/GaN HEMTs. The power gain cut-off frequency gets a peak at the gate voltages from -1.0 volt to - 0.4 volt

corresponding to different AlGaN doping concentrations of GaN/AlGaN/InN/GaN HEMTs. Here, maximum obtained F_T/F_{max} is 726/892 GHz. So, GaN/AlGaN/InN/GaN is suitable for high frequency applications.

4.4. Effect of AlGaN doping concentration on DC and RF performances of HEMTs with inserted atomic layers

According to Fig. 11 and Fig. 12, the drain current is higher for higher AlGaN doping concentration of GaN/AlGaN/AlN/GaN HEMT at any particular combination of drain voltage and gate voltage[15, 16]. According to Fig. 13, the transconductance is higher for larger AlGaN doping concentration of GaN/AlGaN/AlN/GaN HEMT at any particular gate voltage corresponding to the fixed drain voltage (V_d) of 5 volt. According to Fig. 14, the current gain cut-off frequency (F_T) is higher for larger AlGaN doping concentration of GaN/AlGaN/AlN/GaN HEMTs at any particular gate voltage corresponding to the fixed drain voltage (V_d) of 5 volt. According to Fig. 15, the power gain cut-off frequency (F_{max}) is higher for larger AlGaN doping concentration of GaN/AlGaN/AlN/GaN HEMTs at any particular gate voltage corresponding to the fixed drain voltage (V_d) of 5 volt.

According to Fig. 17 and Fig. 18, the drain current is higher for higher AlGaN doping concentration of GaN/AlGaN/InN/GaN HEMT at any particular combination of drain voltage and gate voltage[15, 16]. According to Fig. 19, the transconductance is higher for larger AlGaN doping concentration of GaN/AlGaN/InN/GaN HEMT at any particular gate voltage corresponding to the fixed drain voltage (V_d) of 5 volt. According to Fig. 20, the current gain cut-off frequency (F_T) is higher for larger AlGaN doping concentration of GaN/AlGaN/InN/GaN HEMTs at any particular gate voltage corresponding to the fixed drain voltage (V_d) of 5 volt. According to Fig. 21, the power gain cut-off frequency (F_{max}) is higher for larger AlGaN doping concentration of GaN/AlGaN/InN/GaN HEMTs at any particular gate voltage corresponding to the fixed drain voltage (V_d) of 5 volt.

4.5. Comparative study among HEMT structures of this work

According to the DC analysis of designed HEMTs in this work, the structures with inserted AlN atomic layer have better performance by providing higher drain current and higher transconductance than those of conventional HEMTs at any particular AlGaN doping concentration. Again, structures with inserted InN atomic layer have better DC performance providing higher drain current and higher transconductance than those of structures with inserted AlN atomic layer at any particular AlGaN doping concentration. Hence, HEMT structures with inserted InN atomic layer may be suitable for applications in biomedical sensors with requirements of higher drain current according to the simulation results of this work, at any particular AlGaN doping

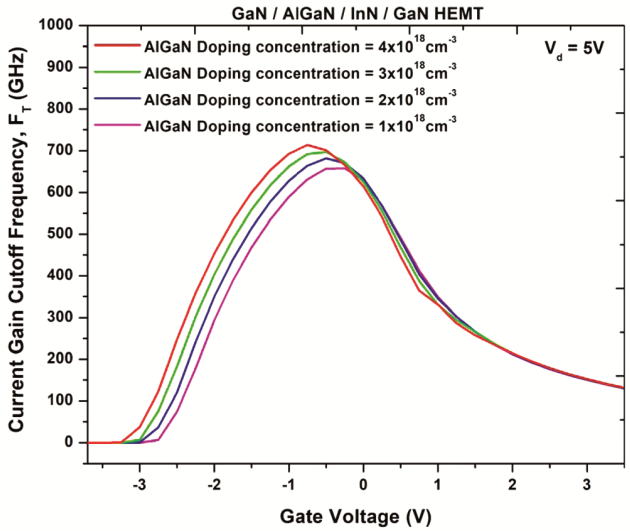

Fig. 20 — The variations in current gain cut-off frequency with gate voltage are shown at the fixed drain voltage (V_d) of 5 volt for different AlGaN doping concentrations corresponding to GaN/AlGaN/InN/GaN HEMTs.

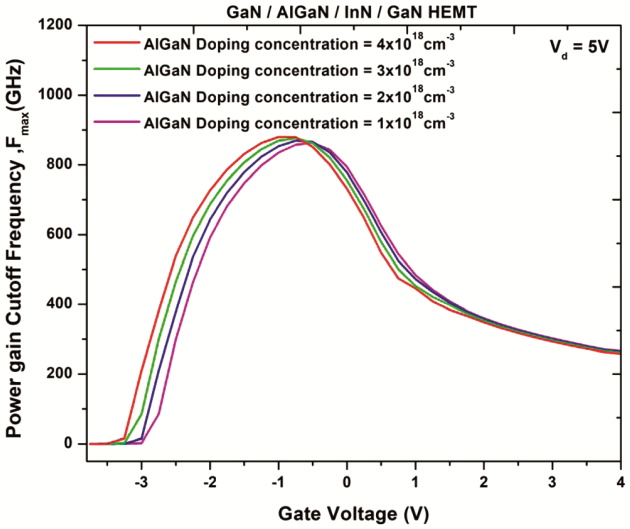

Fig. 21 — The variations in power gain cut-off frequency with gate voltage are shown at the fixed drain voltage (V_d) of 5 volt for different AlGaN doping concentrations corresponding to GaN/AlGaN/InN/GaN HEMTs.

concentration[17-20]. Again, HEMT structures with inserted AlN atomic layer have better RF performance than conventional HEMTs in this work, at any particular AlGaN doping concentration. Also, HEMT structures with inserted InN atomic layer have better RF performance than HEMT structures with inserted AlN atomic layer at any particular AlGaN doping concentration. Therefore, the modified HEMT structures with inserted InN atomic layer may be suitable for high frequency applications according to the simulation results of this work, at any particular AlGaN doping concentration[21, 22].

5 Conclusions

In this work, three individual types of nitride-based Nanoelectronic HEMT structures are designed according to the choice of materials, as follows: (a) conventional GaN/AlGaN/GaN HEMTs, (b) GaN/AlGaN/AlN/GaN HEMTs, and (c) GaN/AlGaN/InN/GaN HEMTs. In each type of these structures, the individually chosen AlGaN doping concentrations are 1×10^{18} cm^{-3}, 2×10^{18} cm^{-3}, 3×10^{18} cm^{-3}, and 4×10^{18} cm^{-3}. The effect of doping concentration on DC and RF performances is systematically investigated according to the simulation results produced by SILVACO-ATLAS physical simulator. The quantum well depth in GaN/AlGaN/InN/GaN HEMT is higher than other two designed structures at any particular AlGaN doping concentration, to produce higher drain current due to higher 2DEG density.

According to the DC analysis, the drain current is highest in GaN/AlGaN/InN/GaN HEMT than other two structures, at the AlGaN doping concentration of 4×10^{18} cm^{-3}. The transconductance is highest in GaN/AlGaN/InN/GaN HEMT among the designed structures, at the AlGaN doping concentration of 4×10^{18} cm^{-3}. Also, according to RF analysis, the current gain cut-off frequency and power gain cut-off frequency are individually highest for GaN/AlGaN/InN/GaN HEMT among the designed structures, at the AlGaN doping concentration of 4×10^{18} cm^{-3}. Therefore, the DC and RF performances are better at higher AlGaN doping concentration. Hence, this work may be suitable in sensor related applications and high frequency applications.

References

1 Charfeddine M, Belmabrouk H, Zaidi M A & Maaref H, *J Mod Phys*, 3 (2012) 881.

2 Chattopadhyay M K & Tokekar S, *Microelectron J*, 39 (2008) 1181.

3 Chattopadhyay M K & Tokekar S, *Solid-State Electron*, 50 (2006) 220.

4 Chattopadhyay M K & Tokekar S, *Microwave Opt Technol Lett*, 49 (2007) 382.

5 Korwal M, Haldar S, Gupta M & Gupta R S, *Microwave Opt Technol Lett*, 38 (2003) 371.

6 Khandelwal S, Goyal N & Fjeldly T A, *IEEE Trans Electron Dev*, 58 (2011) 3622.

7 Khandelwal S, Chauhan Y S & Fjeldly T A, *IEEE Tran Electron Dev*, 59 (2012) 2856.

8 Khandelwal S, Yadav C, Chauhan Y S, Curutchet A, Zimmer T, Jaeger J C D, Defrance N & Fjeldly T A, *IEEE Trans Electron Dev*, 60 (2013) 3216.

9 Khandelwal S & Fjeldly T A, *Solid-State Electron*, 76 (2012) 60.

10 Yigletu F M, Khandelwal S, Fjeldly T A & Iniguez B, *IEEE Trans Electron Dev*, 60 (2013) 3746.

11 Ghosh S, Dasgupta A, Khandelwal S, Agnihotri S & Chauhan Y S, *IEEE Trans Electron Dev*, 62 (2015) 443.

12 Ahsan S A, Ghosh S, Sharma K, Dasgupta A, Khandelwal S & Chauhan Y S, *IEEE Trans Electron Dev*, 63 (2016) 565.

13 Dasgupta A, Khandelwal S & Chauhan Y S, *IEEE Microwave Wirel Comp Lett*, 25 (2015) 376.

14 Khandelwal S, Goyal N & Fjeldly T A, *Solid-State Electron*, 79 (2013) 22.

15 Mukhopadhyay S & Kalita S, *Nano Trends*, 19(1) (2017) 15.

16 Kalita S & Mukhopadhyay S, *J Nanoelectron Optoelectron*, 13 (2018) 1123.

17 Hemaja V & Panda D K, *Silicon*, (2021) https://doi.org/10.1007/s12633-020-00937-w.

18 Tai T Y, Sinha A, Sarangadharan I, Pulikkathodi A K, Wang S L, Shiesh S C, Lee G B & Wang Y L, *Sens Mater*, 30 (2018) 2321.

19 Pal P, Pratap Y, Gupta M & Kabra S, *IEEE Sens J*, 19 (2019) 587.

20 Mishra S N, Saha R & Jena K, *ECS J Solid State Sci Technol*, 9 (2020) 065002.

21 Miao M & Walle C G V D, *Appl Phys Express*, 8 (2015) 024302.

22 Sinha K, Dubey S K & Islam A, *Microsyst Technol*, 26 (2019) 2145.

23 Wuerfl J, Treidel E B, Brunner F, Cho M, Hilt O, Knauer A, Kotara P, Krueger O, Weyers M & Zhytnytska R, *ECS Trans*, 50 (2021) 211.

24 Russo S & Carlo A D, *IEEE Trans Electron Dev*, 54 (2007) 1071.

25 Guo J, Qiu C, Zhu H & Wang Y, *Materials*, 12 (2019) 2653.

26 Lenka T R & Panda A K, *Semiconductors*, 45 (2011) 1211.

27 Yoshikawa A, Che S B, Yamaguchi W, Saito H, Wang X Q, Ishitani Y & Hwang E S, *Appl Phys Lett*, 90 (2007) 073101.

28 Legallais M, Mehdi H, David S , Bassani F, Labau S, Pelissier B, Baron T, Martinez E, Ghibaudo G & Salem B , *ACS Appl Mater Interfaces*, 12 (2020) 39870.

29 Rontu V, Sippola P, Broas M, Ross G, Sajavaara T, Lipsanen H, Paulasto-Krockel M & Franssila S, *J Vac Sci Technol A*, 36 (2018) 021508.

30 Deminskyi P, Rouf P, Ivanov I G & Pedersen H, *J Vac Sci Technol A*, 37 (2019) 020926.

31 Murugapandiyan P, Lakshmi V R, Wasim M & Sundaram K M, *Int J Electron Lett*, 8 (2019) 472.

32 Mohapatra E, Das S, Dash T P, Dey S, Jena J & Maiti C K, *Dev Integr Circuit*, (2019) 326.